Microchimica Acta (2020) 187:193
https://doi.org/10.1007/s00604-020-4167-1

ORIGINAL PAPER

Highly efficient fluorescence sensing of kanamycin using Endo IV-powered DNA walker and hybridization chain reaction amplification

Xiaonan Qu[1] · Jingfeng Wang[2] · Rufeng Zhang[1] · Yihan Zhao[2] · Shasha Li[2] · Yu Wang[2] · Su Liu[1] · Jiadong Huang[2,3] · Jinghua Yu[3]

Received: 2 September 2019 / Accepted: 13 February 2020

Abstract

An ultrasensitive fluorescence sensing strategy for kanamycin (KANA) determination using endonuclease IV (Endo IV)-powered DNA walker, and hybridization chain reaction (HCR) amplification was reported. The sensing system consists of Endo IV-powered 3D DNA walker using for the specific recognition of KANA and the formation of the initiators, two metastable hairpin probes as the substrates of HCR and a tetrahydrofuran abasic site (AP site)-embeded fluorescence-quenched probe for fluorescence signal output. On account of this skilled design of sensing system, the specific binding between KANA and its aptamer activates DNA walker, in which the swing arm can move autonomously along the 3D track via Endo IV-mediated hydrolysis of the anchorages, inducing the formation of initiators that initiates HCR and the following Endo IV-assisted cyclic cleavage of fluorescence reporter probes. The use of Endo IV offers the advantages of simplified and accessible design without the need of specific sequence in DNA substrates. Under the optimal experimental conditions, the fluorescence biosensor shows excellent sensitivity toward KANA detection with a detection limit as low as 1.01 pM (the excitation wavelength is 486 nm). The practical applicability of this strategy is demonstrated by detecting KANA in spiked milk samples with recovery in the range of 98 to 102%. Therefore, this reported strategy might create an accurate and robust fluorescence sensing platform for trace amounts of antibiotic residues determination and related safety analysis.

Keywords DNA nanomachines · Signal amplification · Endonucleases IV · Aptamer · Antibiotic

Introduction

Kanamycin (KANA), as a member of the aminoglycoside antibiotics, exhibits a strong inhibiting ability against Gram-negative bacteria, which has been widely used for treating bacterial infections, mastitis, and pneumonia [1–4]. However, excessive KANA can cause potential side effects including ototoxicity and nephrotoxicity, posing a serious threat to human health [5, 6]. Therefore, it is urgent to construct sensitive and specific assay methods to monitor KANA in foodstuff.

A variety of techniques including high-performance liquid chromatography (HPLC) [7], capillary electrophoresis (CE) [8], gas chromatography-mass spectrometry (GS-MS) [9], and enzyme-linked immunosorbent assay (ELISA) [10] have been developed for KANA identification. Although these techniques are capable of quantitative assay of KANA with high sensitivity and specificity, they may suffer from the shortcomings of laborious sample preparation steps and long

Electronic supplementary material The online version of this article (https://doi.org/10.1007/s00604-020-4167-1) contains supplementary material, which is available to authorized users.

✉ Su Liu
stu_lius@ujn.edu.cn

[1] School of Water Conservancy and Environment, University of Jinan, Jinan 250022, People's Republic of China

[2] School of Biological Sciences and Technology, University of Jinan, Jinan 250022, People's Republic of China

[3] Key Laboratory of Chemical Sensing & Analysis in Universities of Shandong, college of Chemistry and Chemical Engineering, University of Jinan, Jinan 250022, People's Republic of China

Published online: 02 March 2020

analysis time. Therefore, it is desirable to explore convenient strategies for KANA determination with higher sensitivity and low detection limit.

Benefiting from the well-defined Watson-Crick [11] base pairing, DNA can be employed as building blocks for the artificial machineries, such as DNA motors [12], walkers, robots [13], and tweezers [14], which is driven by the thermodynamics embodied in oligonucleotides hybridization. In particular, DNA walkers [15], one of the automated molecular machines that are composed of smart synthetic DNA, have aroused extensive interest of researchers in biosensing fields. Previous studies have shown various DNA walking machines, including one-dimensional (1D), two-dimensional (2D), and three-dimensional (3D) structures, have been designed that can be activated by different activators. For example, Tian et al. report a DNA nanodevice that autonomously moves along a one-dimensional DNA track powered by DNA enzyme [16]. Yang et al. design a DNA nanomachine built from DNA-functionalized gold nanoparticles, which moves along the 3D tracks powered by the nicking endonuclease. Compared to 1D and 2D track, 3D DNA walking machines have been demonstrated to possess better amplification performance due to roomy walking space, excellent DNA enrichment ability, and the resistance of the nonspecific interactions as a result of the use of the large surface area nanoparticles as the substrate. Although the widespread applications in various analytes determination including nucleic acids, proteins, and small molecules, the construction of 3D DNA walkers has never been studied in antibiotics detection until now.

To achieve amplified detection of trace amounts of analytes, signal amplification tools have gained increasingly attention. Such as nucleic acid amplification techniques including rolling circle amplification (RCA) [17, 18], strand displacement amplification (SDA) [19], hybridization chain reaction (HCR) [20–22], catalyzed hairpin assembly (CHA) [23], and polymerase chain reaction (PCR) [24, 25]. Among them, because of its prominence of isothermal, enzyme-free reaction and high amplification efficiency, HCR represents a highly programmable DNA polymerization process induced by an initiator (single-stranded DNA). The system is comprised of a pair of metastable and complementary hairpin probes (HPs) that can be activated and assembled into a long double-stranded DNA product only in the presence of the initiator. Specifically, in the absence of the initiator, these kinds of HPs can stably coexist in the system to acquire low background or eradicate the false positive results.

Inspired by these, we construct an ultrasensitive fluorescence strategy for KANA detection using endonuclease IV (Endo IV)-powered DNA walker and HCR amplification. The specific recognition between KANA and its aptamer activates the 3D DNA walker, in which the swing arm can move autonomously along the 3D track via Endo IV-mediated hydrolysis of the anchorages, inducing the formation of initiators that initiates HCR and the following Endo IV-assisted cyclic cleavage of fluorescence reporter probes. To the best of our knowledge, this work is the first time that the 3D DNA walker coupled with HCR amplification has been used for antibiotics determination. In our assay, a sequence-independent endonuclease, Endo IV, is used to power the constructed 3D DNA walker and catalyze the cyclic cleavage of fluorescence probes. The use of Endo IV offers the advantages of simplified and accessible design without the need of specific sequence in DNA substrates. Additionally, just because of the specific binding of KANA and its aptamer, large amounts of initiators are formed that initiates HCR and the following Endo IV-assisted cyclic cleavage of reporter probes, thus improved specificity and sensitivity can be achieved for KANA determination. Therefore, this Endo IV-assisted dual-amplified strategy might create a convenient, accurate, and ultrasensitive fluorescence sensing platform for detecting trace amounts of analytes in bioanalysis and molecular diagnosis.

Experimental section

Materials and reagents

All oligonucleotides listed in Table 1 were HPLC-purified and synthesized by Sangon Biotechnology Co. Ltd. (Shanghai, China; https://www.sangon.com/). Kanamycin (KANA), streptomycin (SM), gentamicin (GM), ampicillin (AM), tetracycline (TC), chloroauric acid ($HAuCl_4{\cdot}4H_2O$), and trisodium citrate ($Na_3C_6H_5O_7{\cdot}2H_2O$) were supplied by Aladdin Chemistry Co., Ltd. (Shanghai, China; http://www.aladdin-e.com/). The Endonuclease IV (Endo IV) and NEBuffer 3 were purchased from New England Biolabs Inc. (Beijing, China; http://www.neb-china.com). All other reagents were of analytical grade and purchased from Sinopharm Chemical Reagent Co., Ltd. (Beijing, China; https://www.sinoreagent.com/). All solutions were prepared using ultrapure water with resistivity > 18.25 MΩ cm, which was obtained through a Millipore Milli-Q water purification system (Billerica, MA, USA; http://www.merckmillipore.com/). Acryl/bis 30% solution (29: 1), N, N, N′, N′-tetramethylethylenediamine (TEMED), ammonium persulfate, 10 × TBE buffer, and DNA ladder marker (20–300 bp) were purchased from Sangon Biotechnology Co. Ltd. (Shanghai, China; https://www.sangon.com/).

The X highlighted in red in anchorage (AR) and fluorescence-quenched probe (FQP) is the tetrahydrofuran abasic site mimic (AP site), which is the recognition site for Endo IV. The FQP is labeled with 4-(4-dimethylaminophenyl) diazenylbenzoic acid (Dabcyl) quencher and fluorescein isothiocyanate (FAM) fluorophore. The sequence in bold of AR indicates the HCR initiator sequence.

Table 1 DNA oligonucleotides sequence used in this work

Oligonucleotides name	Sequence description (5′ to 3′)
SW	SH-T_{33}TCTTAGCCTCAACCATCATC
AR	SH-TTTTTCACTTGATGATGGXTGA**GAATAAAGTGTTTAAGTA**
Ap	TGGGGGTTGAGGCTAAGCCGAC
HP1	AGGAGTGTTTAAGTTGAAGAATAGTACTTAAACACTTTATTCTTGAGGA
HP2	AGGAGTCTATCTTCAACTTAAACTAGAATAAAGGTGTTTAAGTTGAGGA
FQP	TCCT (Dabcyl)CAAXT(FAM)CCT

Apparatus

Fluorescence spectra were recorded using an Agilent Cary Eclipse spectrofluorometer (Agilent, USA; www.agilent.com) with excitation at 486 nm. The slit was set to be 5 nm for both the excitation and the emission. Absorption spectra were conducted on a UV2600 UV-vis spectrophotometer (Shimadzu international trading Co. Ltd., Japan; http://www.shimadzu.com.cn/) at room temperature. Transmission electron microscopy (TEM) measurements were carried out using a JEM-3010 transmission electron microscope (http://www.jeol.co.jp/). Polyacrylamide gel electrophoresis (PAGE) was performed using a DYCZ-24DN electrophoresis cell (LIUYI, Beijing, China; http://www.zg17w.cn/brand/beijingliuyi.html) and Bio-Rad Gel imaging system (Bio-Rad, USA; http://www.bio-rad.com/).

Analytical protocol

The detailed procedure was as follows: The 3D DNA nanomachines (2 μL, 10 nM), HP1 (2 μL, 2 μM), HP2 (2 μL, 2 μM), NEBuffer 3 (2 μL, 1 ×), Endo IV (1 μL, 5 U μL^{-1}), KANA (2 μL, different concentrations from 0 to 500 nM: 0, 5 pM, 10 pM, 50 pM, 100 pM, 500 pM, 1 nM, 5 nM, 1 nM, 50 nM, 100 nM, and 500 nM), and 7 μL of ultrapure water were mixed at 37 °C for 2 h. Then, FQP (2 μL, 10 μM) was added into the reaction solution at 37 °C for 30 min. Subsequently, the above mixture was added to ultrapure water (80 μL) and scanned using an Agilent Cary Eclipse spectrofluorometer. Unless noted otherwise, all experiments for KANA measurements were repeated three times in this work.

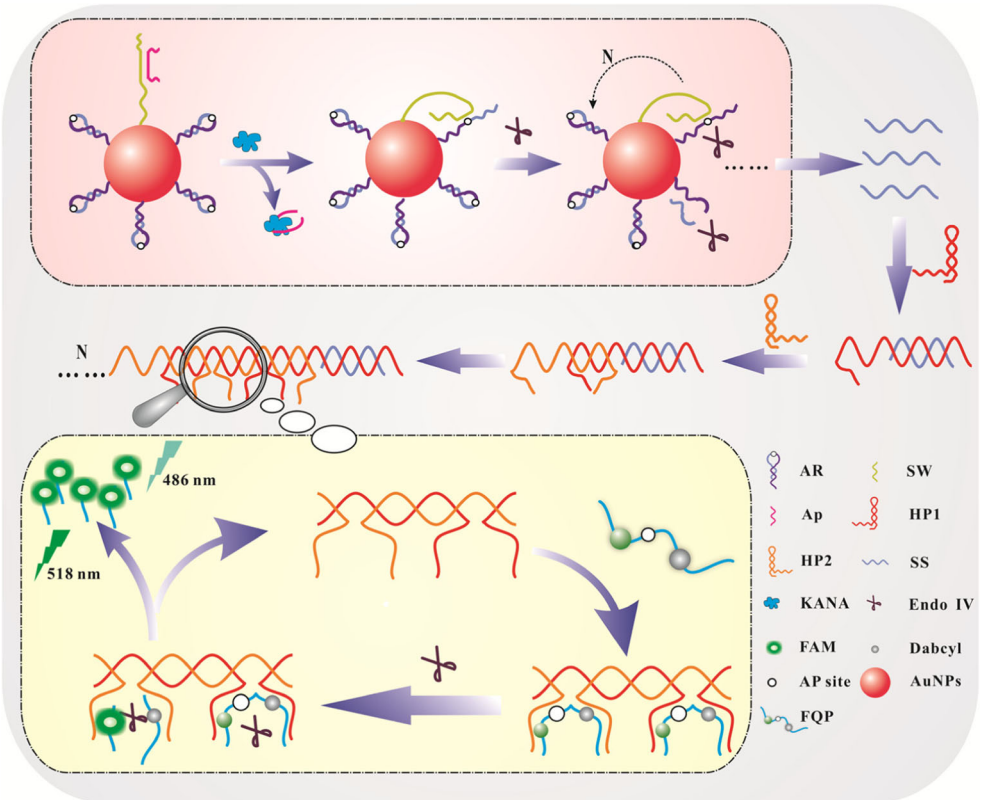

Scheme 1 Schematic illustration of ultrasensitive fluorescence sensing of KANA using the Endo IV-powered DNA walker and HCR amplification.

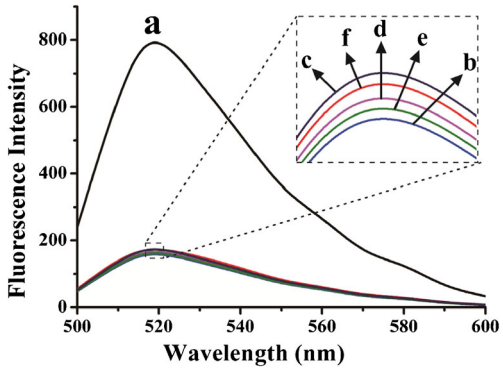

Fig. 1 Fluorescence emission spectra responses of this assay obtained upon analyzing 500 nM KANA (**a**). Curves *b* to *f* were for the feasibility research of the strategy, which was controlled with no KANA (**b**), no Endo IV (**c**), no SW (**d**), no AR (**e**), and no HP1 (**f**)

Results and discussion

Design of the strategy for ultrasensitive determination of KANA

The working principle of the fluorescence sensing strategy is schematically illustrated in Scheme 1. The sensing system consists of Endo IV-powered 3D DNA walker using for the specific recognition of KANA and the formation of the initiators, two metastable hairpins (HP1, HP2) as the substrates of HCR, and a tetrahydrofuran abasic site (AP site)-embeded fluorescence-quenched probe (FQP) for fluorescence signal output. The 3D DNA walker is anchorage (AR) and swing arm (SW) functionalized 20 nm-sized gold nanoparticle (AuNP). AR is a hairpin with a stem-loop structure that an AP site for Endo IV is contained in the loop. Specially, a blocker DNA (anti-KANA aptamer, Ap) is introduced to block SW to efficiently avoid the hybridization of AR with SW. In this design, the 3D DNA walker can be activated via the specific recognition of KANA and its aptamer. With the introduction of target KANA, the specific binding between Ap and KANA leads to the release of SW; thus, SW is able to combine to the loop region of AR and form AP site-contained duplex DNA that can be nicked by Endo IV. So, the 3D DNA walker is activated, in which SW move autonomously along the AuNP surface through cleaving one AR at each step with the aid of Endo IV, and stopped until all cleavages is completed. After the cleavage process via Endo IV-powered 3D DNA walker, a great many of single-stranded DNA (SS) are liberated, which can act as initiators for initiating HCR assembly. SS primarily attaches with the toehold and stem region of HP1, opening the hairpin and exposing the 5′ end of HP1. Immediately, the exposed 5′ end combines with the toehold and stem region of HP2; thus, HP2 is unfolded in which the exposed 3′ terminus enable to hybridize with HP1. In this sense, the cross-opening of HP1 and HP2 induces the formation of polymer chains consisting of the cross-interacting hairpins, in which the protruding tail at the 3′ end of HP1 is in close proximity to the tail at the 5′ terminus of HP2; thus, FQP is able to anneal with the two tails and form stable DNA duplex containing AP site. Subsequently, the Endo IV nicked the site, resulting in the breakage of FQP and followed by the dissociation away from the tails. Another FQP can combine to the two tails, initiating a new cyclic of "hybridization-cleavage" reaction. After Endo IV-assisted cyclic cleavage reaction, numerous FQP is cleaved; thus, the significantly enhanced fluorescence signal is achieved due to the detachment of fluorophore (FAM) from quencher (Dabcyl). In contrast, when KANA is absent in the system, since the two tails in HP1 and HP2 are hidden in the stem due to the metastable structure, the hybridization of FQP with HP1 and HP2 is impossible; thus, a very weak fluorescence signal is obtained due to the FRET phenomenon between FAM and Dabcyl. Hence, the constructed Endo IV-powered DNA walker and HCR amplification strategy holds great potential for analyzing KANA with highly sensitivity and specificity.

Feasibility of this strategy

To verify the feasibility of this strategy, a series of control experiments were performed (Fig. 1). In the presence of

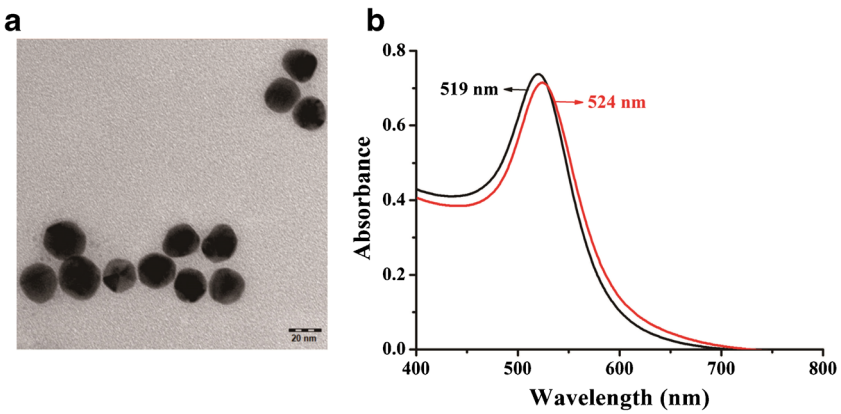

Fig. 2 **a** TEM micrograph of the bare AuNPs; **b** UV-Vis spectra of the bare AuNPs (black curve) and the 3D DNA nanomachines (red curve)

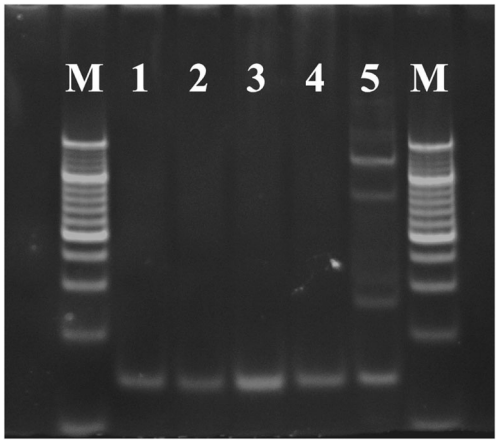

Fig. 3 Gel electrophoresis images. Lane M, DNA marker; Lane 1, HP1; Lane 2, HP2; Lane 3, KANA, DNA nanomachines, Endo IV, and HP1; Lane 4, KANA, DNA nanomachines, Endo IV, and HP2; Lane 5, KANA, DNA nanomachines, Endo IV, HP1, HP2, and FQP

500 nM KANA, a significantly strong fluorescence intensity was obtained at 518 nm (curve *a*). In contrast, a hardly negligible fluorescence intensity was observed without KANA (curve *b*). This indicated that the specific binding of KANA to the aptamer was the mechanism that triggered the release of fluorescent signal. In the absence of Endo IV (curve *c*), low fluorescence intensity was observed. This suggested that the AP site in single-stranded probe was not nicked by the Endo IV which was specific to the AP site-inserted DNA duplex. Additionally, the unconspicuous fluorescence responses almost approximate to that of the blank sample were obtained in the absence of SW and AR (curve d and curve e), respectively; clearly revealing that the HCR products were generated by the combination of the SW and AR. Finally, control without HP1 resulted in non-fluorescent flag (curve *f*), revealing that HP1 participated in HCR process as a vital element. These above results clearly suggested that this assay could be applied for ultrasensitive determination of KANA.

Characterization of the bare AuNPs and the 3D DNA walker

Transmission electron microscopy (TEM) and UV-Vis spectroscopy were utilized to investigate the prepared AuNPs and the 3D DNA nanomachines. It was observed from Fig. 2b that the bare AuNPs with spherical structure exhibited good dispersion and homogeneous size (~ 20 nm diameter). As shown by UV-Vis spectroscopy in Fig. 2b, the bare AuNPs had a strong absorption peak at 519 nm (black curve), while the absorption peak of the 3D DNA nanomachines displayed an obvious red shift to 524 nm [26, 27], demonstrating the successful modification of DNA probes on AuNPs surface (red curve).

PAGE analysis

In order to explore the progress of the HCR reaction, it could be directly characterized by PAGE, and the results were shown in Fig. 3. Lane M represented a DNA marker (20–300 bp). Lane 1 and lane 2 showed the bright bands of HP1 and HP2, respectively. Compared with lane 1, there was an increased brightness in lane 3, which illustrated that a great many of SS were liberated and primarily hybridize with the HP1 after the cleavage process via the Endo IV-powered 3D DNA walker, whereas lane 4 had the basically same brightness as lane 2, which indicated that produced SS could not bind to HP2. It was reasonably concluded that SS produced by the Endo IV-powered 3D DNA walker could be the HCR initiator in the aid of HP1 and HP2. As seen from lane 5, a bright band with a large molecular weight product via HCR process. These results above signified that the HCR reaction was successfully carried out and generated an amplification gain for achieving the ultrasensitive determination of KAMA.

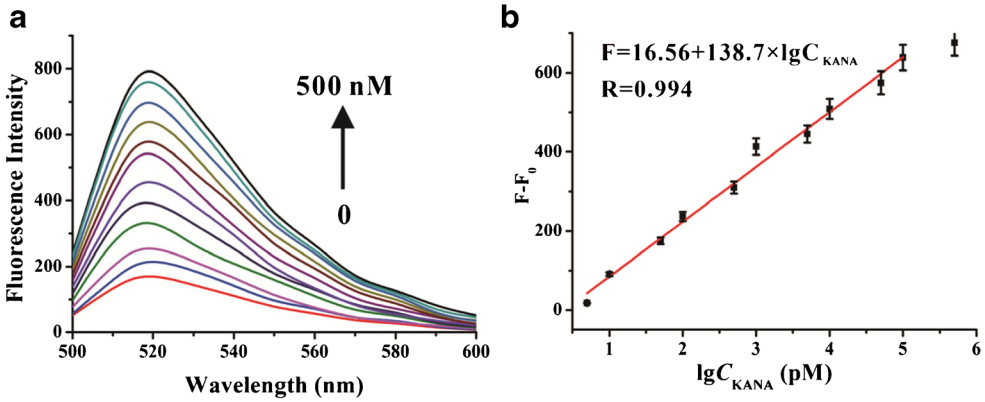

Fig. 4 **a** Fluorescent responses to the different concentrations of KANA (from 5 pM to 500 nM: Blank, 5 pM, 10 pM, 50 pM, 100 pM, 500 pM, 1 nM, 5 nM, 1 nM, 50 nM, 100 nM, 500 nM); **b** The calibration plot for KANA determination based on fluorescent intensity at 518 nm. F and F_0 were the fluorescence intensity at 518 nm in the presence and absence of KANA, respectively. The excitation wavelength was 486 nm. The emission spectra are recorded in the wavelength range from 500 to 600 nm. Error bars were standard deviations across three repetitive experiments

Table 2 An overview on the previously reported nanomaterial-based methods for KANA determination

Materials	Methods	Detection limit (pM)	Reference
TiO_2-MoS_2 nanocomposite	Photoelectrochemical	5.00×10^1	[28]
Single-walled carbon nanohorn	Cyclic voltammetry	1.00×10^5	[29]
Nanofibers	SERS	7.50×10^2	[30]
Carbon nanoparticles	Switch-on FRET	9.00×10^0	[31]
Gold nanoparticles	Colorimetric	1.00×10^2	[32]
Gold nanoparticles	Spectrophotometric	1.00×10^3	[33]
No	Luminescent	1.43×10^2	[34]
TiO_2 nanotube arrays	Photoelectrochemical	1.00×10^2	[35]
Gold nanoparticles	Fluorescence	3.21×10^2	[36]
Gold nanoparticles	Fluorescence	1.01×10^0	this work

Optimization of experimental conditions

To obtain an optimal analytical performance of the fluorescent assay, some parameters were successively investigated by fluorescence spectroscopy: (a) the concentration of DNA nanomachines; (b) the concentration of FQP; (c) the amount of Endo IV; and (d) the reaction time. Respective text and figures on optimizations are given in the Electronic Supporting Material. In short, the following experimental conditions were found to give best results: (a) optimal concentration of DNA nanomachines, 10 nM; (b) optimal concentration of FQP, 10 μM; (c) optimal concentration of Endo IV, 5 U μL^{-1}; and (d) optimal reaction time, 120 min.

Analytical performance of the KAMA assay

In order to demonstrate the analytical performance of this strategy for the KANA assay, we examined the fluorescence emissions of KANA at different concentrations under the optimal conditions. As shown in Fig. 4a, it was found that the fluorescence intensities increased with increasing of the concentrations of KANA, suggesting the fluorescence signal output was highly dependent on the KANA concentration. A linear correlation between the fluorescence intensities at 518 nm and the logarithm of the KANA concentrations ranging from 5 pM to 100 nM was obtained (Fig. 4b). The linear regression equation was $F\text{-}F_0 = 16.56 + 138.7 \times \lg C_{KANA}$ (pM) with a correlation coefficient of 0.994. The limit of detection (LOD) was calculated to be 1.01 pM in terms of the rule of three times standard deviation over the blank response. And, the detailed comparison of the analytical performance between our assay and other earlier reported methods was illustrated in Table 2. It was clearly found that the sensitivity of our assay was superior to the majority of existing methods. These results indicated the studied strategy that might be used for KANA quantification.

Specificity of the assay

The specificity of our reported method was evaluated by introducing different antibiotics, including streptomycin (SM), gentamicin (GM), ampicillin (AM), tetracycline (TC), and kanamycin (KANA). As shown in the Fig. 5, a significant fluorescent intensity was obtained only in the presence of KANA, whereas the responses to nontarget antibiotics were comparable to that of blank sample. These results suggested that the method had admirable specificity for ultrasensitive detection of KANA owing to the specific and stable binding of the aptamer and target.

Practical application

In order to truly validate the practical applicability of this sensor, the quantitative assay of KANA in spiked milk samples was considered. Different concentrations of KANA were added to the milk samples diluted with buffer, and tested directly without any pre-treatment. And, samples added with KANA were also detected by the classical enzyme-linked immunosorbent assay (ELISA) and compared with the results obtained by our constructed strategy. As shown in Table S1, it was observed that the results measured by our assay showing good agreement with the ELISA results, and the discrepancies between the two methods was less than 11.2%. The recovery of this assay was in the range of 98 to 102%. This clearly showed that our method has high reliability and accuracy, and it can be used for the analysis of actual samples.

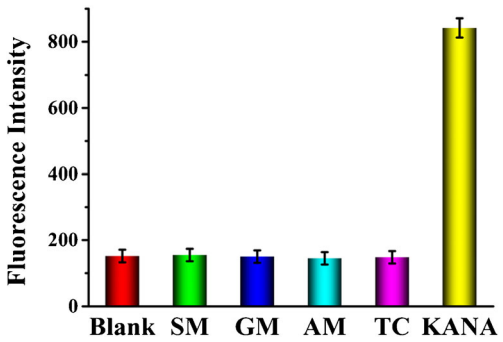

Fig. 5 Specificity evaluation of the fluorescence assay for KANA. The concentration of KANA was 500 nM. The concentrations of the nontarget were 50 μM. Error bars were standard deviations across three repetitive experiments

Conclusions

An efficient and ultrasensitive fluorescence sensing platform for KANA quantification is constructed based on the Endo IV-powered 3D DNA walker and HCR amplification. To the best of our knowledge, this work is the first time that the 3D DNA walker coupled with HCR amplification has been used for antibiotics determination. In our assay, the use of Endo IV offers the advantages of simplified and accessible design without the need of specific sequence in DNA substrates. In addition, improved specificity and sensitivity can be achieved for KANA determination due to the combination of 3D DNA walker and HCR amplification. It is noteworthy that the analysis cost could be reduced by replacing the dual-labeled fluorescence probes by the specific fluorescence dyes (e.g., N-methyl mesoporphyrin IX and Thioflavin T). Under the optimal experimental conditions, the results reveal the constructed fluorescence biosensor shows excellent sensitivity toward KANA detection with a detection limit as low as 1.01 pM. Furthermore, the practical applicability of this strategy is demonstrated by detecting KANA in spiked milk samples with satisfactory recovery in the range of 98 to 102%. Therefore, the constructed fluorescence biosensor might provide a useful and practical tool for trace amounts of antibiotic residues determination and related safety analysis.

Funding information This work was supported by National Natural Science Foundation of China (31471644), the Primary Research & Development Plan of Shandong Province (2017GSF220009) and the Program for Taishan Scholer of Shandong Province (TS201712048).

Compliance with ethical standards

Conflict of interest The author(s) declare that they have no competing interests.

References

1. Chen ZC, Xiong F, Yu AM, Lai GS (2019) Aptamer biorecognition-triggered DNAzyme liberation and Exo III-assisted target recycling for ultrasensitive homogeneous colorimetric bioassay of kanamycin antibiotic. Chem Commun 55:3959–3662
2. Bai Z, Chen Y, Li F, Zhou Y, Yin H, Ai S (2019) Electrochemical aptasensor for sulfadimethoxine detection based on the triggered cleavage activity of nuclease P1 by aptamer-target complex. Talanta 204:409–414
3. Liao QG, Wei BH, Luo LG (2017) Aptamer based fluorometric determination of kanamycin using double-stranded DNA and carbon nanotubes. Microchim Acta 184:627–632
4. Robati RY, Arab A, Ramezani M, Langroodi FA, Abnous K, Taghdisi SM Aptasensors for quantitative detection of kanamycin. Biosens Bioelectron 82:162–172
5. Zeng RJ, Zhang LJ, Luo ZB, Tang DP (2019) Palindromic fragment-mediated single-chain amplification: an innovative mode for photoelectrochemical bioassay. Anal Chem 91:7835–7841
6. Zhang K, Gan N, Shen ZP, Cao JX, Hu FT, Li TH (2019) Microchip electrophoresis based aptasensor for multiplexed detection of antibiotics in foods via a stir-bar assisted multi-arm junctions recycling for signal amplification. Biosens Bioelectron 130:139–146
7. Mcwhinney BC, Wallis SC, Tara H, Roberts JA, Jeffrey L, Ungerer JPJ (2010) Analysis of 12 beta-lactam antibiotics in human plasma by HPLC with ultraviolet detection. J Chromatogr B 878:2039–2043
8. Liu JX, Zhao MZ, Deng Y, Tie C, Chen HX, Zhou YL, Zhang XX (2013) The coating of smart pH-responsive polyelectrolyte brushes in capillary and its application in CE. Electrophoresis 34:1352–1358
9. Turner NW, Subrahmanyam S, Piletsky SA (2009) Analytical methods for determination of mycotoxins: a review. Anal Chim Acta 632:168–180
10. Wenxiao J, Zhanhui W, Beier RC, Haiyang J, Yongning W, Jianzhong S (2013) Simultaneous determination of 13 fluoroquinolone and 22 sulfonamide residues in milk by a dual-colorimetric enzyme-linked immunosorbent assay. Anal Chem 85:1995–1999
11. Watson TL, Pearson J, Clifford CWG (2004) Perceptual grouping of biological motion promotes binocular rivalry. Curr Biol 14:1670–1674
12. Cha TG, Pan J, Chen HR, Salgado J, Li X, Mao CD, Choi JH (2014) A synthetic DNA motor that transports nanoparticles along carbon nanotubes. Nat Nanotechnol 9:39–43
13. Yaniv A, Eldad BI, Daniel L, Shmulik I, Almogit AH, Ido B (2014) Universal computing by DNA origami robots in a living animal. Nat Nanotechnol 9:353–357
14. Liu M, Fu J, Hejesen C, Yang Y, Woodbury NW, Gothelf K, Liu Y, Yan H (2013) A DNA tweezer-actuated enzyme nanoreactor. Nat Commun 24:2127
15. Zhao L, Sun R, He P, Zhang X (2019) Ultrasensitive detection of exosomes by target-triggered three-dimensional DNA walking machine and exonuclease III-assisted electrochemical ratiometric biosensing. Anal Chem 91:14773–14779
16. Tian Y, He Y, Chen Y, Yin P, Mao C (2005) A DNAzyme that walks processively and autonomously along a one-dimensional track. Angew Chem Int Ed 44:4355–4358
17. Yao Q, Wang YQ, Wang J, Chen SM, Liu HY, Jiang ZR, Zhang XE, Liu SM, Yuan Q, Zhou X (2018) An ultrasensitive diagnostic biochip based on biomimetic periodic nanostructure-assisted rolling circle amplification. ACS Nano 12:6777–6783
18. Song W, Zhang Q, Sun W (2015) Ultrasensitive detection of nucleic acids by template enhanced hybridization followed by rolling circle amplification and catalytic hairpin assembly. Chem Commun 51:2392–2395
19. Zhang HG, Li FY, Chen HL, Ma YH, Qi SD, Chen XG, Zhou L (2015) AuNPs colorimetric sensor for detecting platelet-derived growth factor-BB based on isothermal target-triggering strand displacement amplification. Sensor Actuat B-Chem 207:748–755
20. Gu Y, Song J, Li MX, Zhang TT, Zhao W, Xu JJ (2017) Ultrasensitive microRNA assay via surface plasmon resonance responses of Au@Ag nanorods etching. Anal Chem 89:10585–10591
21. Wu Z, Liu GQ, Yang XL, Jiang JH (2015) Electrostatic nucleic acid nanoassembly enables hybridization chain reaction in living cells for ultrasensitive mRNA imaging. J Am Chem Soc 137:6829–6836
22. Zhang K, Cao JX, Wu YX, Hu FT, Li TH, Wang Y, Gan N (2019) A fluorometric aptamer method for kanamycin by applying a dual amplification strategy and using double Y-shaped DNA probes on a gold bar and on magnetite nanoparticles. Microchim Acta 186:120
23. Xue C, Zhang SX, Ouyang CH, Chang D, Salena BJ, Li Y, Wu ZS (2018) Target-induced catalytic assembly of Y-shaped DNA and its application for in situ imaging of microRNAs. Angew Chem Int Ed 57:9739–9743

24. Manzanares-Palenzuela CL, De-Los-Santos-Álvarez N, Lobo-Castañón MJ, López-Ruiz B (2015) Multiplex electrochemical DNA platform for femtomolar-level quantification of genetically modified soybean. Biosens Bioelectron 68:259–265
25. Lee NY (2018) A review on microscale polymerase chain reaction based methods in molecular diagnosis, and future prospects for the fabrication of fully integrated portable biomedical devices. Microchim Acta 185:22
26. Xu C, Zhang F, Wang K, Xu E, Liu Y, Wei W et al (2019) A three-dimensional DNAzyme motor for sensitive imaging of telomerase activity in living cells. Sensor Actuat B Chem 298:126930
27. Cryer AM, Chan C, Eftychidou A, Maksoudian C, Mahesh M, Tetley TD, Spivey AC, Thorley AJ (2019) Tyrosine kinase inhibitor gold Nanoconjugates for the treatment of non-small cell lung cancer. ACS Appl Mater Interfaces 11:16336–16346
28. Liu X, Liu P, Tang Y, Yang L, Li L, Qi Z et al (2018) A photoelectrochemical aptasensor based on a 3D flower-like TiO2-MoS2-gold nanoparticle heterostructure for detection of kanamycin. Biosens Bioelectron 112:193–201
29. Han S, Li B, Song Z, Pan S, Zhang Z, Yao H et al (2016) A kanamycin sensor based on an electrosynthesized molecularly imprinted poly-o-phenylenediamine film on a single-walled carbon nanohorn modified glassy carbon electrode. Analyst 142:218–223
30. Nguyen TA, Park S, Kim JB, Kim TK, Seong GH, Choo J et al (2011) Polycrystalline tungsten oxide nanofibers for gas-sensing applications. Sensors Actuators B Chem 160:549–554
31. Wu Z, Hui L, Liu Z (2015) An aptasensor for carcinoembryonic antigen based on upconversion fluorescence resonance energy transfer. Biosens Bioelectron 206:531–537
32. Chong KC, Thang LY, Quirino JP, Hong HS (2017) Monitoring of vancomycin in human plasma via portable microchip electrophoresis with contactless conductivity detector and multi-stacking strategy. J Chromatogr A 1485:142
33. Zhou N, Zhang J, Tian Y (2014) Aptamer-based spectrophotometric detection of kanamycin in milk. Anal Methods 6:1569
34. Leung KH, He HZ, Chan SH, Fu WC, Leung CH, Ma DL (2013) An oligonucleotide-based switch-on luminescent probe for the detection of kanamycin in aqueous solution. Sensor Actuat B-Chem 177:487–492
35. Xin Y, Li Z, Zhang Z (2015) Photoelectrochemical aptasensor for the sensitive and selective detection of kanamycin based on Au nanoparticle functionalized self-doped TiO2 nanotube arrays. Chem Commun 51:15498–15501
36. Ramezani M, Danesh NM, Lavaee P, Abnous K, Taghdisi SM (2016) A selective and sensitive fluorescent aptasensor for detection of kanamycin based on catalytic recycling activity of exonuclease III and gold nanoparticles. Sensor Actuat B-Chem 222:1–7